Oil-Forced Versus Oil-Directed Cooling of Power Transformers

Marko Sorgic and Zoran Radakovic

***Abstract*—In this study, an analysis of the oil-forced (OF) and oil-directed (OD) cooling of oil power transformers was performed. The starting point was a case study of an OF transformer with a declared rated power of 360 MVA having thermal problems in operation. The effects of possible improvements of the cooling were analyzed, where the limiting factor was the geometry of the transformer (winding, core, and tank); cross sections and cooling channels of the windings and the core were also resolved. All calculations, showing an influence of varying characteristics of the cooling (the pump, the cooler, modification from OF to OD construction), were realized with software based on a detailed thermal-hydraulic model. This method gives all relevant oil flows (including oil bypass between the winding and the tank) and all temperatures for a specified configuration and specified parameters of the cooling system. Based on the results, the limits of OF cooling in general are clearly described in this paper. Finally, the effect of applying oil guiding elements inside the windings is illustrated and discussed.**

***Index Terms*—Hot-spot temperature, oil bypass, oil-directed (OD) cooling, oil-forced (OF) cooling, thermal design, transformer.**

I. Introduction

THE temperature in oil power transformers is the most important limiting factor for their loading. Consequently, a very important issue in the transformer industry is to have an efficient cooling system. This means designing a cooling system to meet the required temperature rise limits while minimizing the overall cost. Producers of transformers usually perform optimization of thermal design based on the experience gained from previously produced and tested transformers. This approach, through the use of empirical factors, ensures robustness but is strongly limited to similar transformers produced in the past. For an essential step forward in thermal design, the calculation methods based on physics (fundamentals of heat and mass transfer) are required.

There are standards (for example, [1]) with specified thermal tests and allowable limits for the temperature rises of the top oil and average winding. The temperature of the winding hot spot is the data commonly specified in the purchasing contract. In reality, certain safety margins have to be applied during the design (i.e., the temperature obtained by the calculation has to be somewhat lower than the allowed temperature rises). If the producers do not possess enough knowledge and proper tools, they typically increase the safety margins and consequently cannot approach close to the allowed temperature rises. The statistics of deviations of the measured from the guaranteed temperature limits, and subsequent financial consequence, are exposed in [2]—these results clearly show the importance of developing and applying modern high-quality tools for accurate thermal calculation during a design process. These days, a detailed thermal-hydraulic model is accepted by the experts as a platform for these modern tools. The basic postulates of the theory can be found in [3]–[5]. In our previous paper [6], the complete methodology (basics given in Section II) is explained. The developed method covers all cooling modes and is fully integrated (a closed loop for inner heating and outer cooling).

This paper represents the natural continuation of paper [6] and gives examples of the application of the method. The examples given in this paper were initialized by a case study of a transformer with OF cooling, 360 MVA, having thermal problems in operation. The essence of the proposed reconstruction of the transformer is to reduce the oil bypass, caused by inappropriate (too strong) pumps. Further papers will focus on the verification of the model—the calculated temperatures will be compared with the measured temperatures (average winding, mixed top oil, bottom oil, and the ones obtained with the fiber-optics technique inside the active part of transformer: local oil and on the insulation of the conductor).

Sections III and IV provide basic information about the original construction of the transformer. Section V contains hydraulic networks for OF and OD cooling arrangements; the considered option for the reconstruction of the transformer is also discussed in this section, while the calculation results are given in Section VI.

Based on the calculation results, a general consideration of OF cooling and its comparison with OD cooling are contained in Sections VII and VIII. In addition to the effect of guiding the oil into the windings (OD cooling), the effect of the introduction of zigzag oil inside the winding is illustrated in one example.

II. Thermal-Hydraulic Model in Brief

Our previous paper [6] gives the basics of detailed THM. Hydraulic networks are made for each part of a transformer, while thermal networks are established for the parts where losses exist. These networks contain much fewer elements and nodes than models using the finite-elements method (FEM)—for example, each turn of the winding is represented by one node in the thermal network.

One of the results of solving these networks is the pressure dropping across the parts of a transformer and the oil temperatures at the points where the oil exits a transformer part. The

Manuscript received December 14, 2009; revised March 15, 2010 and April 21, 2010; accepted June 09, 2010. Date of publication August 26, 2010; date of current version September 22, 2010. Paper no. TPWRD-00924-2009.

The authors are with the Faculty of Electrical Engineering, University of Belgrade, Belgrade 11000, Serbia (e-mail: radakovic@etf.rs; sorgic@etf.rs).

Color versions of one or more of the figures in this paper are available online at http://ieeexplore.ieee.org.

Digital Object Identifier 10.1109/TPWRD.2010.2053391

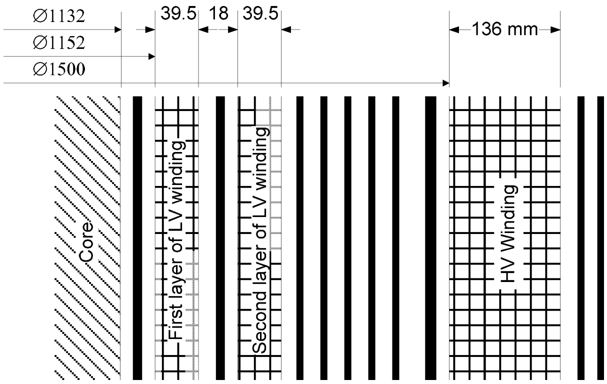

Fig. 1. Radial dimensions.

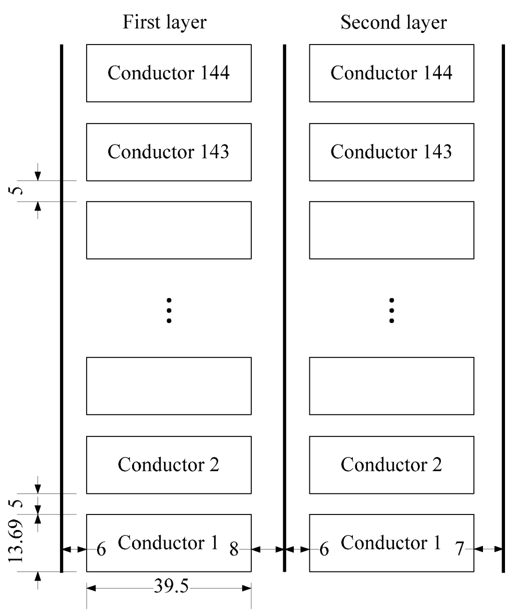

Fig. 2. Low-voltage (LV) winding.

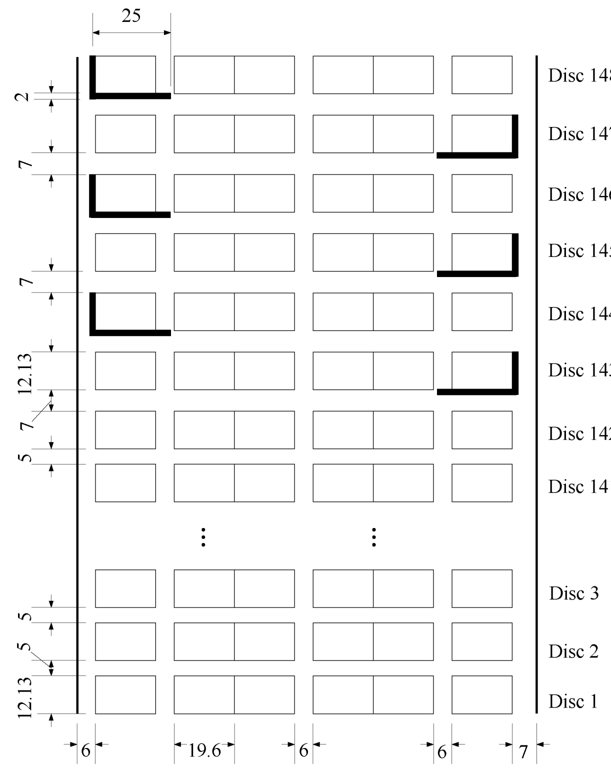

Fig. 3. High-voltage (HV) winding.

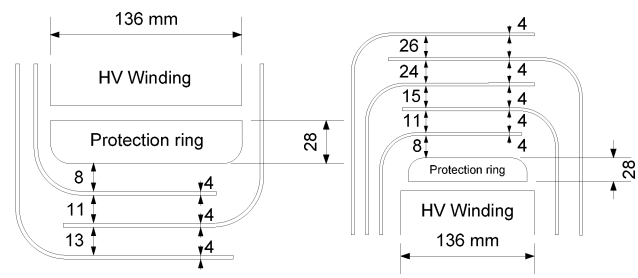

Fig. 4. Insulation system below and above the HV winding.

sum of the pressure drops across each closed oil loop is equal to the calculated produced pressure (due to the thermal driving force and the pumps). These components are dependent on the oil flows through the transformer parts. The oil flows are calculated in the main iterative calculation loops. The final criterion is that the produced pressure is in equilibrium with the pressure drops across each of the closed oil loops. In addition, the oil temperature at the exit of the last part in the loop has to be equal to the assumed oil temperature at the inlet to the first transformer part in the loop.

The final result of the method is a detailed description of the oil flow throughout a transformer (all of the oil flows through each part and its distribution in the oil channels inside the parts) and a detailed description of the oil and conductor temperatures. Thus, the method delivers the position of the hot-spot temperature and its temperature.

The inputs for the calculation are the distribution of the power losses at specified temperature, the construction of the transformer (geometry), and the characteristics of the applied materials.

One of the major benefits of the method is that it is deeply rooted in physics and responds to change of any detail in the construction or change of the material (for example, the oil type). The method also considers relevant aspects of practical production, such as bulging of paper insulation, reducing the radial cooling channels during winding (they become smaller than the designed value). From a practical point of view, it is also important that the design software have an appropriate data base of the equipment (for example: fans, pumps, coolers, tubes, etc.).

III. Data About Transformer

This section contains the major constructive data of the transformer (three-phase five-limb, 360 MVA, 235 kV/15 kV, YNd5, short-circuit voltage 12.46%): the radial dimensions (Fig. 1), the low-voltage winding LV (Fig. 2), high-voltage HV winding (Fig. 3) and insulation systems above and below the HV winding (Fig. 4).

The data about compact cooler—will be designated as Cooler 1 (the cooling system consists of five identical coolers): rated power 180 kW, rated oil flow 60 m^3/h, rated hot-oil temperature

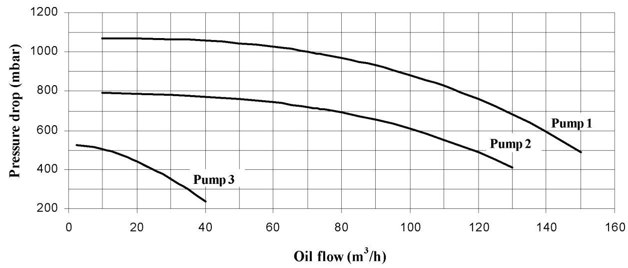

Fig. 5. Characteristic of the oil pumps.

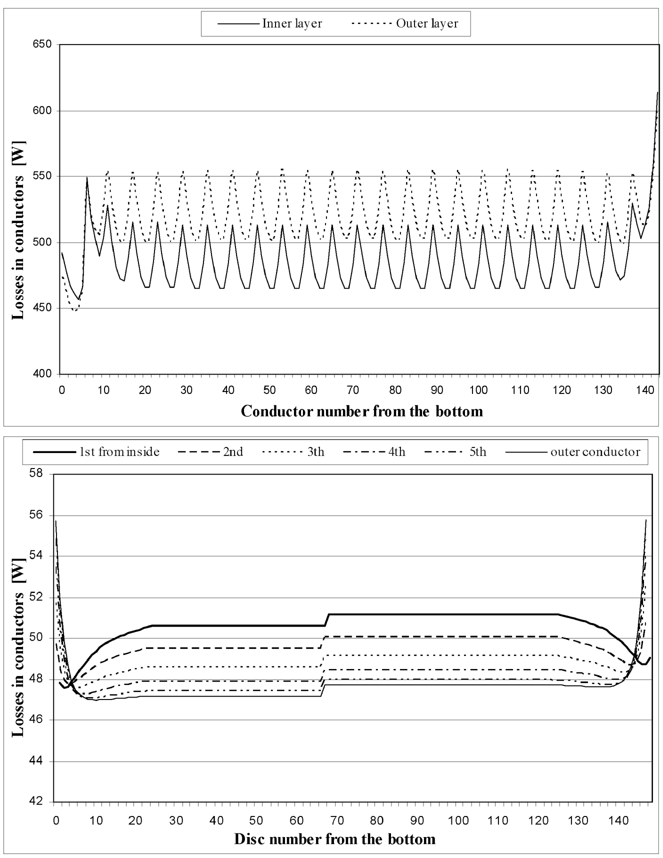

Fig. 6. Distribution of the power losses in the windings.

85 °C, rated cold oil temperature 78.8 °C, rated pressure drop 398 mbar, rated air flow 8.0 m^3/s, rated cold air temperature 40 °C, and rated heated air temperature 61.1 °C.

Each cooler has its own pump, with the characteristics of "Pump 1" given in Fig. 5.

IV. Power Losses

The total losses amount to load losses—in the HV and LV windings at a rated load of 935 kW and no-load losses—in the core 210 kW. The distribution of the power losses in the windings is shown in Fig. 6. The smaller losses at the bottom of the LV windings are the consequence of the shorter turns in the region of the transition from the inner to the outer layer (six conductors leave the layer at $1/6, 2/6, \ldots, 6/6$ of the circumference).

The core consists of five limbs, with windings on the three main limbs (Fig. 7). For the core, the oil flows through four

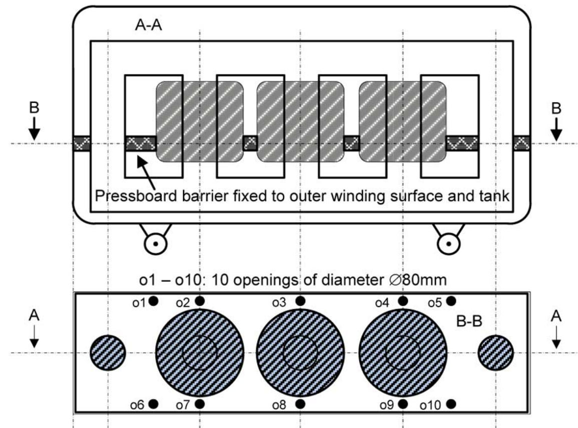

Fig. 7. Implementation of an oil barrier for reducing oil bypass.

parallel paths: 1) parallel main limbs, including the yoke parts below and above the main limbs—three branches; 2) parallel yokes between the main limbs—two branches; 3) parallel return limbs, including the yoke parts below and above the return limb—two branches; and 4) parallel yokes between the main and return limbs—two branches. The total losses are distributed over these core parts according to their geometry and estimated magnetic field.

The method also treats heat transfer on the tank surfaces. The losses in the tank cover (3 kW), floor (3 kW), each of the longer walls (3 kW), and each of the shorter walls (1 kW) represent their rough approximation, and were taken to be constant (i.e., independent of the oil temperature). The losses in the tank walls are small and they have no noticeable influence on the oil flows and oil temperatures calculated by the model.

V. Case Studies and Hydraulic Networks

As stated, the transformer was built as an OF construction and had serious thermal problems. The transformer was produced in 1981 and from the very beginning, analysis of the gas in the oil showed increasing amounts of hydrogen and methane (after 15 years, hydrogen was 100–200 ppm and methane 100–250 ppm); also, ethylene was high (more than 400 ppm). In 1999, there was an electrical breakdown. During repair in the factory, the LV windings were replaced with new ones. In February 2007, it again went into normal operation in the thermal power station. Diagnostics showed an enormous increase in furans (2-FAL): during the first year from 0.46 ppm to 7.41 ppm; the humidity was high from the beginning—it increased during the first year from 47 ppm to 53 ppm (at 66 °C). In the following six months, high values for hydrogen and methane, and extremely high humidity were recorded. Reconditioning of the oil was performed permanently in order to maintain the breakdown voltage (it was falling to 100 kV/cm). In August 2008, the decision was made to take the transformer out of service and perform factory repairs again. The degree of polymerization of the paper at different positions of the HV winding was below 260; at the top of the HV winding, it was below 180.

Before performing the repair, the decision was made to examine the possibility of improvements of the complete cooling system. The limitation was to keep the existing geometry of

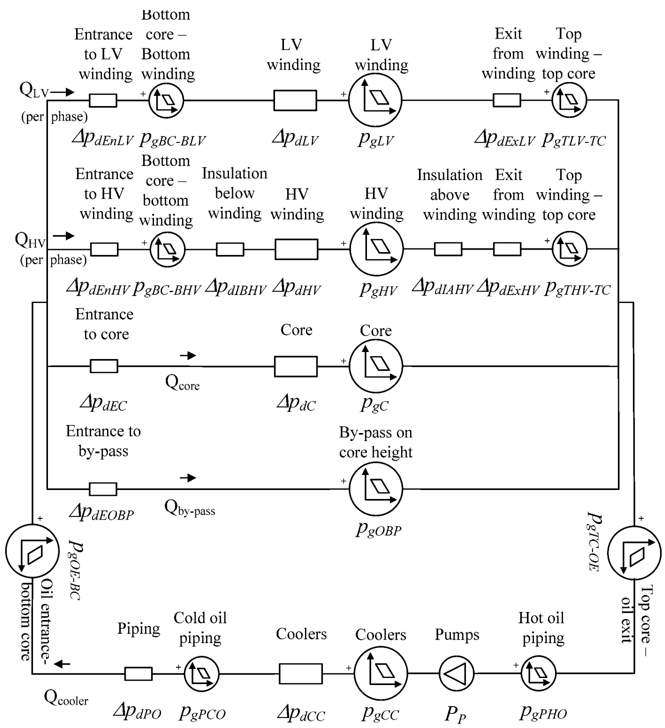

Fig. 8. Hydraulic network of the OF configuration.

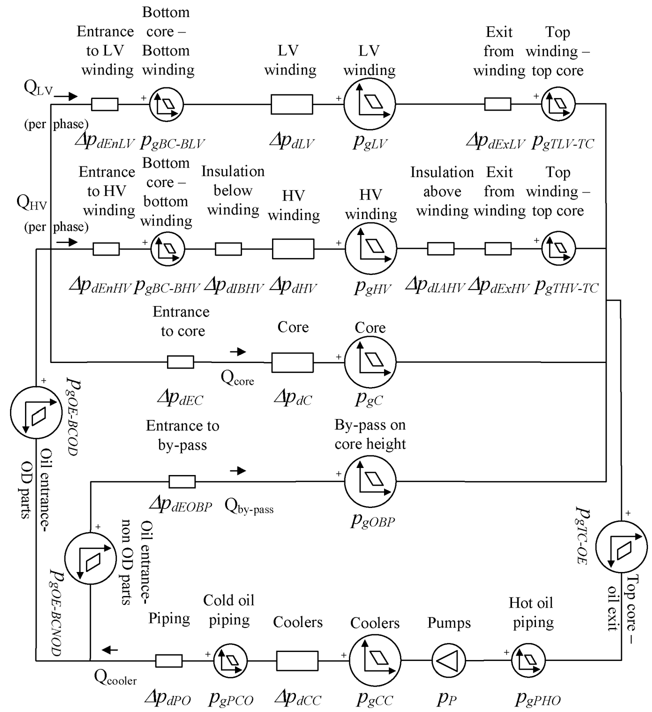

Fig. 9. Hydraulic network of an OD configuration with flow to free space.
p_g—component of gravitational pressure;
Δp_d—component of pressure drop (frictional and local);
Q—oil flow (m^3/h).

Key:
- CC—cooler (in this case, a compact oil to air cooler);
- HV—high-voltage windings from bottom to top;
- LV—low-voltage windings from bottom to top;
- OBP—oil bypass at a height from the bottom to the top of the core;
- C—core from bottom to top;
- TC-OE—from the top of the core to the exit of oil from the tank;
- PHO—pipes for hot oil;
- P—pump;
- PCO—pipes for cold oil;
- PO—complete pipes for oil;
- OE-BC—from the exit of the oil from the cooler to the bottom of the core (for the case of OF cooling);
- EOBP—entry to the oil bypass;
- EC—entry to the core;
- EnW—entry to the winding;
- BC-BW—from bottom of the core to the bottom winding;
- IBW—insulation below the winding;
- W—winding (LV or HV);
- IAW—insulation above the winding;
- ExW—exit from the winding (under pressing ring);
- TW-TC—from the top of the winding to the top of the core;
- OE-BCOD—from the entry of the oil to the tank to the bottom of the core for OD-cooled parts;
- OE-BCNOD—from the entry of the oil to the tank to the bottom of the core for non-OD-cooled parts.

the windings, core, and tank (i.e., not to change the construction of these elements). Thermal calculations were performed for the following cases: 1) the original construction; 2) smaller pumps; 3) a barrier (table) with openings (Fig. 7) to reduce oil bypass through the space between the windings and the tank; 4) larger coolers; 5) barrier with openings + larger coolers; and 6) a barrier, but with complete sealing (completely preventing oil bypass).

Fig. 8 shows the hydraulic network for the OF configuration and Fig. 9 shows the hydraulic network for the OD configuration (both windings and the core are OD cooled and there are openings enabling the oil to flow to the free space—between the windings and the tank). The network of the OD configuration when oil flow to the free space is prevented (complete sealing—case f)) is the same as the network in Fig. 9, but without a branch with flow $Q_{\text{by-pass}}$.

Control calculations were made to verify the method: the results for the OF and the OD configuration with a large number of openings to the free space (100) of diameter 100 mm were almost the same.

It should be mentioned that with usual OD constructions, there are holes under the windings which are used to adjust the distribution of oil flows between the windings. These holes did not exist in the configurations considered for the reconstruction of the transformer.

A representation of the global distribution of oil flow and characteristic oil temperatures for OF cooling were given in [6] while it is presented in Fig. 10 for OD cooling. Figs. 9 and 10 are given for standard OD constructions, with an oil distribution channel transporting oil from the entrance to the tank to the OD-cooled elements (windings, core).

It is interesting to note that the components $p_{g\,\text{OE-BC OD}}$ and $p_{g\,\text{OE-BC NOD}}$ by OD cooling slightly differed due to the slight difference in the temperatures of the oil entering the OD-cooled elements $(\vartheta_{bo,r})$ and the oil entering the non-OD-cooled elements and the oil bypass $(\vartheta_{bo,\text{mix}})$. The oil entering the OD-cooled elements is the oil exiting the cooler. The mixture of oils with temperatures $\vartheta_{bo,r}$ and $\vartheta_{bo,t}$, after heat exchange with the bottom part of the walls (below the pipe from the cooler) and with the floor of the tank, enters the non-OD-cooled elements and the oil bypass.

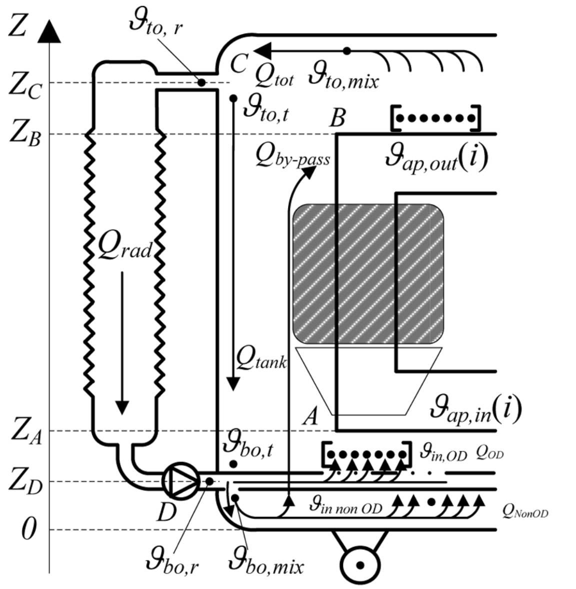

Fig. 10. Global oil flow for OD cooling with flow allowed to the free space.
$Q_{\rm rad}$: oil flow through the coolers (radiators, that is, compact coolers) (m^3/s);
$Q_{\rm tank}$: oil flow downward the tank (m^3/s);
$Q_{ap\,i}$: oil flow through each of active parts (windings and core) (m^3/s);
$Q_{\rm by-pass}$: oil flow in the space between the windings and the tank (bypass of oil) (m^3/s);
$Q_{\rm tot}$: total oil flow (m^3/s);
$Q_{\rm tot} = Q_{\rm rad} + Q_{\rm tank} = \sum(Q_{ap\,i}) + Q_{\rm by-pass}$;
$\vartheta_{bo,r}$: temperature of the oil exiting the cooler (°C);
$\vartheta_{bo,t}$: temperature of the oil at the tank bottom, at the height of the pipe from the cooler (°C);
$\vartheta_{bo,\rm mix}$: temperature of a mixture of oils of temperatures $\vartheta_{bo,r}$ and $\vartheta_{bo,t}$ (°C);
$\vartheta_{\rm in\,OD}$: temperature of oil entering the OD-cooled parts (°C);
$\vartheta_{\rm in\,non\,OD}$: temperature of the oil entering the non-OD-cooled parts (°C);
$\vartheta_{ap,\rm out}(i)$: temperature of the oil exiting each of the active parts (°C);
$\vartheta_{\rm to,mix}$: temperature of mixed oil—a mixture of oils exiting the active parts and the oil bypass (°C);
$\vartheta_{{\rm to},r}$: temperature of the oil entering the radiators (°C);
$\vartheta_{{\rm to},t}$: temperature of the oil at the top of tank, at the height of the pipe to the cooler (°C).

There is a variety of other practical topologies, all being treated and described by the corresponding mass and heat balance equation. Examples: 1) OD arrangement without oil flow to the free space and 2) OD arrangement with non-OD-cooled elements (core and/or regulating windings, for example), high losses in the tank walls, and oil near the tank walls flowing upwards. The pictures of oil distribution for some of them will be published in further publications dealing with practical aspects of the utilization of the developed method in thermal design.

One fundamental theoretical background that is used throughout the analyses in this paper is the method for the calculation of the cooling power and pressure drop in the compact cooler under conditions differing from those rated (rated hot-oil temperature, cold air temperature, oil flow and air flow). It is based on rated data for the cooler and starts from well-known equations for heat exchangers [7], in which the resistance to conductive heat transfer is neglected. It is assumed that thermal resistances to convective heat transfer on the oil side and on the air side are equal at rated operating conditions. The

TABLE I
TOPOLOGIES FOR THE CALCULATED CASES

Case	Pump (see Figure 5)	Number of holes	Diameter of holes (mm)	Cooler	Zigzag oil flow
Original	Pump 1	OF	OF	Cooler 1	No
Case 1	Pump 2	OF	OF	Cooler 1	No
Case 2	Pump 3	OF	OF	Cooler 1	No
Case 3	Pump 1	20	100	Cooler 1	No
Case 4	Pump 1	15	100	Cooler 1	No
Case 5	Pump 1	10	100	Cooler 1	No
Case 6	Pump 1	10	80	Cooler 1	No
Case 7	Pump 1	OF	OF	Cooler 2	No
Case 8	Pump 1	10	80	Cooler 2	No
Case 9	Pump 1	OF	OF	Cooler 3	No
Case 10	Pump 1	10	80	Cooler 3	No
Case 11	Pump 1	Sealed	Sealed	Cooler 1	No
Case 12	Pump 1	Sealed	Sealed	Cooler 1	Yes

TABLE II
RATED DATA CONCERNING THE COOLERS

	Power (kW)	Oil flow (m^3/h)	Pressure drop (mbar)	Cold oil (°C)	Hot air (°C)
Cooler 1	180	60	398	78.8	61.1
Cooler 2	240	65	636	77.4	64.4
Cooler 3	300	80	618	77.2	62.4

calculation of cooling power under conditions differs from the rated runs through the calculation of convection heat-transfer coefficients (α). They depend on the flow and temperature. The functional dependences from the literature are rearranged to the forms without geometry factors; forms are based on the ratios: $\alpha/\alpha_r = f(Q/Q_r, \vartheta/\vartheta_r)$. This approach was necessary since the detailed construction of a heat exchanger is, as a rule, unknown. A similar procedure was applied for the calculation of the pressure drop, for which basic expressions for the pressure drop for oil flow through the tubes are used.

The data concerning the topologies for each of the calculations (cases) are given in Table I. Cases 3–6, 8, and 10 are with OD cooling. A sketch of the OD cooling achieved by the implementation of a pressboard oil barrier with 10 openings, each of 80 mm diameter, is shown in Fig. 7. Case 12 (zigzag oil flow) was achieved by positioning the barriers in the LV windings: they are positioned in such a way that there were always 8 parallel radial channels in the zigzag oil flow; only the last pass had 7 parallel radial cooling channels (thus, there were 17 passes with 8 radial cooling channels and one pass with 7 radial channels). The characteristics of the cooler (rated temperature of the hot oil was 85 °C and for cold air, it was 40 °C) are shown in Table II.

VI. CALCULATION RESULTS

For all 13 specified cases, thermal calculations were realized assuming an ambient temperature of 25 °C and using rated load conditions.

Tables III–VI show the pressures on each element of the hydraulic networks shown in Figs. 8 and 9. These values enabled the pressure equilibriums in the transformer to be understood. Only the sum of the components of the gravitational pressure over the complete closed loops (according to Fig. 8, that is, Fig. 9) is the value which can be meaningfully compared with

TABLE III
PRESSURE OF THE PUMP AND COMPONENTS OF THE GRAVITATIONAL PRESSURE (p_g) IN THE COMMON BRANCH (MBAR)

	P	TC-OE	PHO	CC	OE-BC	OE-BCOD	OE-BCNOD
Orig.	926.0	152.3	215.9	205.7	61.35	/	/
Case 1	612.4	151.8	215.2	205.2	61.22	/	/
Case 2	236.4	150.6	213.6	203.9	60.96	/	/
Case 3	926.2	152.2	215.8	205.7	/	61.34	61.35
Case 4	926.2	152.2	215.8	205.7	/	61.34	61.35
Case 5	926.3	152.2	215.8	205.7	/	61.34	61.35
Case 6	926.4	152.2	215.8	205.7	/	61.34	61.35
Case 7	980.9	153.1	118.2	305.9	61.73	/	/
Case 8	981.0	153.1	118.2	305.9	/	61.72	61.73
Case 9	932.9	153.9	118.8	307.4	62.01	/	/
Case 10	933.4	153.9	118.8	307.4	/	62.00	62.01
Case 11	926.3	152.2	215.8	205.6	/	61.33	63.41
Case 12	926.2	152.2	215.8	205.6	/	61.33	63.41

The gravitational pressure in the PCO is zero as the height at both its ends is the same

TABLE IV
COMPONENTS OF THE GRAVITATIONAL PRESSURE (Δp_g) IN THE BRANCHES (MBAR)

	BC-BLV	LV	TLV-TC	BC-BHV	HV	THV-TC	C	OBP
Orig.	58.70	220.7	50.36	63.75	205.5	59.39	330.5	331.3
Case 1	58.58	220.2	50.27	63.63	205.1	59.28	329.9	330.6
Case 2	58.33	219.3	50.07	63.36	204.3	59.05	328.5	329.2
Case 3	58.69	220.9	50.47	63.74	205.7	59.56	330.7	331.3
Case 4	58.69	221.0	50.50	63.74	205.7	59.61	330.8	331.0
Case 5	58.69	221.0	50.54	63.74	205.8	59.67	330.8	331.3
Case 6	58.69	221.1	50.57	63.74	205.8	59.73	330.9	331.4
Case 7	59.06	222.0	50.64	64.15	206.8	59.73	332.5	333.4
Case 8	59.05	222.4	50.83	64.14	207.1	60.02	332.9	333.4
Case 9	50.84	222.9	50.84	59.97	207.7	59.97	333.9	334.9
Case 10	59.32	223.4	51.10	64.43	208.1	60.36	334.4	334.9
Case 11	58.68	221.2	50.62	63.73	205.9	59.82	330.9	-
Case 12	58.68	221.3	50.63	63.73	205.9	59.79	330.9	-

TABLE V
COMPONENTS OF THE PRESSURE DROP (Δp_d) IN THE WINDINGS BRANCHES (MBAR)

	EnLV	LV	ExLV	EnHV	IBHV	HV	IAHV	ExHV
Orig.	0	1.432	0.1558	0	0.3183	1.910	0.3567	0.0213
Case 1	0	1.394	0.1610	0	0.3160	1.886	0.3590	0.0219
Case 2	0	1.321	0.1716	0	0.3122	1.839	0.3636	0.0231
Case 3	≈0	1.942	0.2755	≈0	0.4596	2.243	0.5389	0.0362
Case 4	≈0	2.138	0.3304	≈0	0.5171	2.362	0.6137	0.0427
Case 5	≈0	2.442	0.4243	≈0	0.6095	2.540	0.7349	0.0537
Case 6	≈0	2.764	0.5348	≈0	0.7115	2.722	0.8694	0.0665
Case 7	0	1.567	0.1393	0	0.3275	1.994	0.3486	0.0194
Case 8	≈0	2.651	0.3683	≈0	0.6101	2.691	0.7087	0.0479
Case 9	0	1.681	0.1288	0	0.3372	2.065	0.3419	0.0179
Case 10	≈0	3.445	0.4747	≈0	0.7762	3.194	0.8964	0.0608
Case 11	≈0	3.645	0.8987	≈0	1.0226	3.212	1.2508	0.1077
Case 12	≈0	3.057	1.0855	≈0	0.9587	3.110	1.1613	0.1192

The pressure drops in IBLV and IALV are zero since there is no insulation below / above the LV winding

TABLE VI
COMPONENTS OF THE PRESSURE DROP (Δp_d) IN THE OTHER PARTS (MBAR)

	CC	PO	EC	C	EOBP
Orig.	898.5	26.86	0	0.803	0
Case 1	594.0	17.50	0	0.784	0
Case 2	228.9	6.112	0	0.749	0
Case 3	887.7	26.84	0.0014	1.542	0.9558
Case 4	897.4	26.83	0.0020	1.841	1.3022
Case 5	897.0	26.82	0.0030	2.302	1.816
Case 6	896.5	26.81	0.0041	2.785	2.334
Case 7	961.2	19.07	0	0.871	0
Case 8	959.5	19.04	0.0024	2.411	1.8736
Case 9	905.2	27.29	0	0.9298	0
Case 10	902.7	27.22	0.0036	3.375	2.9062
Case 11	895.0	26.80	0.0080	3.212	-
Case 12	895.2	26.81	0.0715	3.845	-

TABLE VII
OIL FLOWS (M^3/H)

	HV windings	LV windings	Core	Oil by-pass	Compact cooler
Orig.	3 x 23.45	3 x 18.09	38.05	293.3	455.9
Case 1	3 x 23.88	3 x 18.26	38.90	199.1	364.4
Case 2	3 x 24.76	3 x 18.62	40.50	46.56	217.2
Case 3	3 x 31.50	3 x 22.70	73.53	219.6	455.7
Case 4	3 x 34.53	3 x 24.37	86.69	192.4	455.7
Case 5	3 x 39.20	3 x 26.89	105.9	151.4	455.6
Case 6	3 x 44.05	3 x 29.47	125.1	109.9	455.5
Case 7	3 x 22.01	3 x 17.47	35.38	227.1	380.9
Case 8	3 x 36.34	3 x 25.85	95.97	98.08	380.6
Case 9	3 x 20.88	3 x 16.96	33.45	300.6	447.6
Case 10	3 x 41.02	3 x 28.90	115.4	121.8	447.0
Case 11	3 x 57.27	3 x 36.40	174.5	-	455.6
Case 12	3 x 62.49	3 x 34.51	164.6	-	455.6

pressure produced by the pump and with the pressure drops on the transformer components. The sign of each gravitational pressure depends on the angle between velocity and gravity vectors [6]. This is described with the orientation of components of gravitational pressure ("+" sign) on Figs. 8 and 9. The meaning of the symbols is given in the legend below Fig. 9.

Table VII presents the oil flows which directly influence the vertical temperature gradients and winding to oil temperature gradients (via the convection heat-transfer coefficients).

Table VIII gives the oil temperatures at the entrance and exit of the transformer parts. The values of $\vartheta_{\mathrm{to,mix}}$ are not presented in the table, since they are less than 0.2 K higher than $\vartheta_{\mathrm{to},r}$, due to the small heat transfer to the tank cover and the part of the tank walls above the pipe to the cooler (see Fig. 10). The highest oil temperature differs from the value $\vartheta_{\mathrm{to,mix}}$, which was measured in a standard heat-run test.

The temperatures (hot spot, being the critical value and average winding, measured in a standard heat-run test) and characteristic values (winding to oil gradient and hot-spot factor) for the LV and HV windings are given in Tables IX and X, respectively. The average winding temperature was calculated from the value of dc resistance of the complete winding, as described in [6]. The location of the hot spot was the same for all calculated cases: for the LV winding at the inner top conductor and for the HV winding at the third conductor in the top disc.

VII. DISCUSSION OF THE RESULTS

A. *Influence of the Oil Pump With OF Cooling*

The first three calculations (Original, Case 1, and Case 2) showed the influence of the size of pump in the OF cooling

TABLE VIII
OIL TEMPERATURES ϑ (°C)

	bo, r	*bo, mix*	*in non OD*	*out LV*	*out HV*	*out core*	*to, r*	*av, r*
Orig.	67.18	67.18	67.01	78.66	84.58	77.76	71.78	69.48
Case 1	69.65	69.49	69.42	80.84	86.77	79.91	75.35	72.50
Case 2	74.98	74.66	74.53	85.49	91.46	84.56	84.37	79.67
Case 3	67.17	67.05	66.94	75.87	81.17	72.77	71.83	69.50
Case 4	67.16	67.05	66.92	75.11	80.20	71.91	71.82	69.49
Case 5	67.17	67.05	66.89	74.17	78.98	71.06	71.84	69.50
Case 6	67.16	67.04	66.82	73.40	78.06	70.46	71.87	69.51
Case 7	59.63	59.52	59.47	71.87	77.82	71.12	65.21	62.42
Case 8	59.63	59.51	59.31	67.24	72.02	63.95	65.30	62.46
Case 9	54.12	54.04	54.00	61.16	73.03	66.29	58.93	56.52
Case 10	54.11	54.03	53.90	60.91	65.40	57.74	59.03	56.57
Case 11	67.41	-	-	72.21	76.25	69.77	72.17	69.79
Case 12	67.41	-	-	71.81	76.73	69.91	72.17	69.79

$\vartheta_{out\,LV}$ Temperature of the oil exiting the LV winding
$\vartheta_{out\,HV}$ Temperature of the oil exiting the HV winding
$\vartheta_{out\,core}$ Temperature of the oil exiting the core
$\vartheta_{out\,oil\,by\text{-}pass}$ Temperature of oil by-pass at the height of the top of the core;
$\vartheta_{out\,oil\,by\text{-}pass} = \vartheta_{in\,non\text{-}OD}$: this is valid when the oil flows downwards in the tank (Q_{tank} in Figure 10 has a positive value); if Q_{tank} would be negative (case of high power losses in the tank), $\vartheta_{bo,\,mix}$ would be equal to $\vartheta_{bo,\,r}$
$\vartheta_{in\,OD} = \vartheta_{bo,\,r}$ (strictly, this is valid for the standard OD construction and is not true for the construction shown in Figure 7; this is also valid for $\vartheta_{in\,non\,OD}$; the practical impact is small and thus the development of a program for the special construction shown in Figure 7 was not worthwhile).
$\vartheta_{av,\,r}$ Average temperature of the oil in the cooler

TABLE IX
CHARACTERISTIC VALUES FOR THE LV WINDING

			Based on $\vartheta_{out\,LV}$		Based on $\vartheta_{to,\,mix}$	
	$\vartheta_{hs\,LV}$	$\vartheta_{av\,LV}$	$\vartheta_{av\,LV}-\vartheta_{ao\,LV}$	$H_{r\,LV}$	$\vartheta_{av\,LV}-\vartheta_{ao,\,mix}$	$H_{s\,LV}$
Orig.	103.8	91.01	18.18	1.385	21.62	1.483
Case 1	105.8	93.14	18.01	1.387	20.75	1.468
Case 2	110.1	97.69	17.68	1.392	18.25	1.411
Case 3	101.3	89.64	18.11	1.404	20.14	1.464
Case 4	100.6	89.21	18.07	1.409	19.71	1.458
Case 5	99.62	88.66	17.99	1.414	19.16	1.450
Case 6	98.76	88.18	17.90	1.417	18.66	1.441
Case 7	97.79	84.46	18.80	1.379	22.12	1.472
Case 8	93.46	82.04	18.60	1.409	19.57	1.439
Case 9	93.57	79.83	19.25	1.372	23.36	1.483
Case 10	87.77	76.49	18.98	1.415	19.92	1.443
Case 11	92.27	87.43	17.62	1.422	17.64	1.423
Case 12	82.16	75.16	5.56	1.864	5.38	1.859

$\vartheta_{ao\,LV}$ Average oil temperature in the LV winding: $(\vartheta_{in\,OD} + \vartheta_{out\,LV})\,/\,2$ (°C)
$\vartheta_{ao,\,mix}$ Average oil temperature: $(\vartheta_{in\,OD} + \vartheta_{to,\,mix})\,/\,2$ (°C)
H_r Real Hot-spot factor of winding 1: $(\vartheta_{hs\,LV} - \vartheta_{out\,LV})\,/\,(\vartheta_{av\,LV} - \vartheta_{ao\,LV})$
H_s Hot-spot factor based on mixed top oil: $(\vartheta_{hs\,LV} - \vartheta_{to,\,mix})\,/\,(\vartheta_{av\,LV} - \vartheta_{ao,\,mix})$

mode. As expected, the oil flow through the windings and the core does not change. When stronger pumps are used, the flow of oil through the bypass and the compact coolers increases. In other words, the windings and the core take the same quantity of oil and using stronger pumps results only in an increase of oil through the bypass.

A strong pump (i.e., oil bypass) causes the temperature of the oil entering the cooler to be lower than the temperatures of oil exiting the windings and the core. This results in a reduction of the temperature of the oil entering the cooler and, consequently, of the cooling power of the cooler. Another important issue is that this can be seriously misleading if loading strategy, monitoring, and protection were based on the temperature of the oil entering the cooler (i.e., on mixed oil under the tank cover).

TABLE X
CHARACTERISTIC VALUES FOR THE HV WINDING

			Based on $\vartheta_{out\,HV}$		Based on $\vartheta_{to,\,mix}$	
	$\vartheta_{hs\,HV}$	$\vartheta_{av\,HV}$	$\vartheta_{av\,HV}-\vartheta_{ao\,HV}$	$H_{r\,HV}$	$\vartheta_{av\,HV}-\vartheta_{ao,\,mix}$	$H_{s\,HV}$
Orig.	106.2	90.86	15.07	1.434	21.47	1.603
Case 1	108.3	93.13	15.03	1.433	20.74	1.589
Case 2	112.9	97.95	14.96	1.432	18.50	1.541
Case 3	102.8	90.08	15.91	1.360	20.58	1.505
Case 4	101.8	89.80	16.11	1.340	20.30	1.476
Case 5	100.5	89.42	16.35	1.315	19.92	1.437
Case 6	99.32	89.08	16.46	1.291	19.56	1.404
Case 7	99.62	83.83	15.19	1.436	21.49	1.601
Case 8	93.72	82.27	16.45	1.319	19.81	1.435
Case 9	95.01	78.80	15.29	1.438	22.33	1.615
Case 10	86.89	76.44	16.69	1.288	19.87	1.402
Case 11	97.13	88.51	16.68	1.252	18.72	1.334
Case 12	97.86	88.84	16.78	1.260	19.05	1.348

The meaning of the symbols is the same as for Table IX, but related to HV winding instead of LV winding

Nevertheless, a stronger pump helps—by using a stronger pump (Original case), there is more oil flow through the compact cooler, and heat transfer from the oil to the cooler surface is improved (the thermal resistances of the oil to the cooler surface and total oil to air—are smaller). The effect is that the average oil-to-air gradient is smaller with a stronger pump (see Table VIII). Although the vertical oil temperature gradient is smaller with a stronger pump (similar transferred power and greater oil flows—the basic equations are given in [6]), the temperature of the bottom oil entering the active parts is lower.

B. Influence of the Barriers for the Prevention of Oil Flow to the Free Space

The calculations of relevance are the Original and Cases 3–6. For Case 6, representing the smallest openings (10 openings with a diameter of 80 mm) and the strongest hydraulic resistance to oil bypass, the oil bypass changes significantly (drops from about 290 m^3/h for OF cooling to about 110 m^3/h). It should be emphasized that the total oil flow (through the coolers) remains the same; consequently, the oil flows through the windings and the core increase. These are the results of the following facts related to the produced pressure and pressure drop: 1) pressure drop: the pressure drop over the cooler is dominant; hence, the change of the pressure drops over the other elements with changing oil flow do not significantly affect the pressure drop over the complete oil loop; 2) The thermal driving force in a closed loop, obtained as the algebraic sum of all gravitational components (for example, Case 1, LV winding $205.2 + 0 + 215.2 + 61.22 - 151.8 - (58.58 + 220.2 + 50.27) = 0.77$ Pa) is small compared to the pressure produced by the pump (612.4 Pa); hence, its change will not affect the total driving force significantly; 3) the change in the thermal driving forces (caused by different oil temperatures resulting from different oil flows) is small; and 4) the pressure drop over the cooler does not change significantly since the finally calculated oil flows and the oil temperatures do not change significantly. Example: results of the calculation for the Original versus Case 6: oil flow through and pressure drop over the cooler 455.9 m^3/h, 898.5 mbar versus 455.5 m^3/h, 896.5 mbar; oil flow and pressure drop through the HV winding 23.45 m^3/h, 1.432 mbar versus 44.05 m^3/h, 2.764 mbar; and pressure produced by the pumps 926 mbar versus 926.4 mbar.

The major benefit of directing a larger quantity of oil into the windings and the core is a reduction of the oil temperature at the top of the winding and the consequential reduction of the hot-spot temperature: original versus Case 6: HV winding 106.2 °C versus 99.32 °C and the LV winding is 103.8 °C versus 98.76 °C.

C. *Influence of Different Compact Coolers*

As shown, preventing oil flow to the free space does not significantly influence the outer cooling. In order to reduce the complete oil temperature level (bottom and top oil), larger coolers should be used. Cases 7 to 10 show the results for two larger coolers, where both calculations, with OF and with 10 openings of 80-mm diameter, were performed (Table I).

The results clearly confirm the effects of directing the oil discussed in Section VII-B. In all previous cases, oil bypass was enabled by making specified holes in the oil barrier. The last two cases (11 and 12) relate to a completely sealed transformer and fully directed oil flow to the windings and core. The results for Case 11 follow the trend of results obtained by reducing the number and diameter of the openings (Cases 3–6).

D. *Influence of Guiding the Oil Through the Winding*

In all previous calculations, the average winding to average oil in the winding temperature gradient did not drop noticeably on increasing the oil flow and oil velocity in the winding. There are two reasons for this. The first is that the convection heat-transfer coefficient depends not only on the oil velocity, but also on the oil parameters [6], [7], where the oil viscosity is very sensitive to temperature changes. The second is that for the existing configuration of cooling channels inside the windings (Figs. 2 and 3), the oil flow has a minor effect on the cooling of horizontal surfaces (radial cooling channels).

From the results obtained in this study, it is obvious that with OD cooling and compact coolers, the pressure drop in the windings is small compared to the other pressure drops. Consequently, zigzag oil flow through the winding [Fig. 11(a)] comes naturally into consideration: with this cooling configuration, a larger pressure drop might be expected, since the oil path through the winding is longer. Zigzag oil flow enables the efficient use of radial cooling channels—without the use of oil barriers in the winding, in radial cooling channels, there is, in fact, a kind of natural oil flow.

Case 12 illustrates the effect of barriers placed in the LV windings. This is the only change with respect to Case 11. Directing of the oil in the HV windings might have been realized by positioning barriers and closing the cooling channels near the cylinders and inside the winding. This type of arrangement can be calculated using the program module for a labyrinth cooling arrangement [Fig. 11(b)].

The effect of changing the construction in the LV winding to zigzag (from Case 11 to Case 12) is a change of the pressure drop and consequential change of the oil flow through the

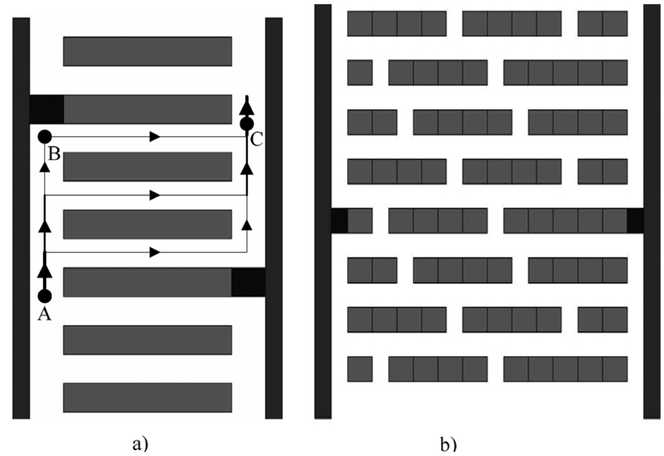

Fig. 11. Windings with barriers for guiding the oil through radial channels. (a) With zigzag oil flow. (b) Labyrinth.

LV winding from 36.4 m^3/h to 34.51 m^3/h (the decrease is relatively small), while the reduction of the average winding to average oil temperature gradient from 17.62 K to 5.56 K, and of the hot-spot from 92.27 °C to 82.16 °C are significant. It is interesting that the introduction of the oil barriers decreased the pressure drop in the winding from 3.645 to 3.057 Pa; the hydraulic resistance (ratio of the pressure drop and the oil flow) decreases from 0.1001 to 0.0886 Pa/(m^3/h). This result will be discussed since it might seem paradoxical. Considering the inner axial cooling channel of the first layer, if there are no barriers (Fig. 2), the oil velocities in the axial channels near each of the conductors are constant moving upwards. When there are barriers [Fig. 11(a)], the oil velocities near the conductors drop moving upwards from the barrier. In the case with the barrier, the total pressure drop is equal to the sum of the pressure drops in the axial channels on the side of the oil entrance (A to B) and the pressure drop in the top radial channel (B to C). This sum is not necessarily greater than the sum of the pressure drops in the axial ducts of the winding without barrier, when the oil velocity is constant from the bottom to the top of the winding. The difference of total pressure drops for the cases with and without barriers depends on the geometry—the number of the radial channels between the barriers, and the width and length of the axial and radial cooling ducts. A hydraulic network for zigzag oil flow is given in [6]. In addition to frictional pressure drops in the windings, there are also local pressure drops. Accurate and reliable equations for determining them have still not been published and represent one of challenges in the development of THM. In order to remain within the frame of common knowledge, the local pressure drops were neglected in the calculations of the results given in this paper.

VIII. OD Versus OF Cooling

OD cooling (oil directed to the windings) enables more efficient cooling. Practically, this means that higher current densities (A/mm^2) can be allowed (i.e., smaller cross sections of the conductor for the same current can be adopted).

If the pump by OF cooling is strong, oil bypass appears, decreasing the temperature of the oil entering the cooler and, in this way, decreasing the efficiency of the cooler. In addition, the temperature of the mixed top oil, also measured in a heat-run test and in real operation, can give bad information (i.e., seriously misleading the customer by the acceptance test and later on in operation). It appears that there is a saturation oil flow through the active part (windings and the core) (i.e., increasing the pump over a certain limit does not lead to an increase in the oil flow through the active part). These oil flows through the windings are low (in the case original construction is 18.09 m^3/h per phase for the LV windings and 23.45 m^3/h per phase for the HV winding); consequently, the vertical temperature gradient (11.48 K for the LV windings and 17.4 K for the HV windings) and the hot-spot temperature are high. These values are, in fact, close to the corresponding ones of a standard transformer with ON cooling.

OD cooling enables much larger oil flows through the windings to be achieved (for Case 11, 36.40 m^3/h per phase for the LV winding and 57.27 m^3/h per phase for the HV winding) and decreasing vertical temperature gradients (4.80 K for the LV windings and 8.84 K for the HV windings) and hot-spot temperatures in the windings. The limitation for OD cooling is, in fact, only the oil velocity, which must not exceed the value causing the generation of static electricity (typically the employed limit in design is 50 cm/s).

The results of the calculations revealed in this paper also indicate that zigzag or labyrinth oil flows are preferable arrangements for OD cooling. The eventual increase of the pressure drop in the winding has a small impact on the complete system (when using compact coolers), while the increases of the convection heat-transfer coefficients in radial cooling channels and the decrease of winding to oil temperature gradients are significant.

The construction which was taken for this case study originated from the practice and the target of the project (the inspiring point for this paper) and was the reconstruction of the cooling from OF to OD. For this reason, a specific construction solution was applied to implement OD cooling (see Fig. 7) and the cooling of the core could have been treated as OD. In practice, the common construction is that there is an oil distribution channel supplying the oil to the windings through holes designed and used to regulate the oil-flow distribution in different windings (the diameter and the length of the holes and the number of the holes can be adjusted). In these cases, OD cooling of the core is not possible. Instead, small openings in the oil distribution channels are left to enable oil leakage for the cooling of the core. The developed method also enables the calculation of this construction.

IX. Conclusion

Starting from a real construction of the 360-MVA OFAF transformer with oil to air compact coolers, this paper analyzed the characteristic thermal parameters in OF and OD cooling modes. The calculations are realized using software based on a detailed thermal-hydraulic model, following the physics of oil flow and heat transfer in each single oil channel and in all parts of the transformer—inside the tank and in the cooler. It is the first published comprehensive application of a model which was introduced in a previous paper [6]. This paper shows the practical potential of the model in analyzing different design options and realizing design optimization.

Although the analyses were initialized by a case study, the final results and conclusions are general, illustrating the limitations of OF cooling and the advantages of OD cooling. The results clearly show the quantity and consequences of oil bypass. In addition, this paper clearly shows the possible danger of wrong conclusions being reached in interpreting the results of a heat-run test and in the estimation of the temperatures during real operation, if mixed top oil under the tank cover is considered as the only relevant top-oil temperature.

This paper indicated the limit of possible oil flow through the active parts by OF cooling. To increase oil flow over this limit, OD cooling has to be applied. The influence of increasing oil flow to oil and winding temperatures was also shown.

The employment of oil barriers for producing zigzag oil flow in the winding does not cause significant changes of the total pressure drops in the oil loops and of the total oil flow (in the case of forced oil circulation and the application of compact coolers). Barriers significantly increase cooling on the surfaces of windings attaching radial cooling channels. Based on this, arrangements with oil guiding elements (zigzag or labyrinth) seem to be optimal for OD transformers with compact coolers.

References

[1] *Power Transformers—Temperature Rise*, IEC Std. 60076-2, 1993.
[2] Z. Radakovic and M. Sorgic, "Wirtschaftliche Betrachtung der thermischen Auslegung von ölgekühlten Leistungstransformatoren," Elektrizitätswirtschaft, vol. 107, no. 15, pp. 32–38, 2008.
[3] K. Karsai, D. Kerényi, and L. Kiss, *Large Power Transformers*. New York: Elsevier, 1987.
[4] A. J. Oliver, "Estimation of transformer winding temperatures and coolant flows using a general network method," *Proc. Inst. Elect. Eng.*, vol. 127, pt. C, pp. 395–405, 1980.
[5] M. Yamaguchi, T. Kumasaka, Y. Inui, and S. Ono, "The flow rate in a self-cooled transformer," *IEEE Trans. Power App. Syst.*, vol. PAS-100, no. 3, pp. 956–963, Mar. 1981.
[6] Z. Radakovic and M. Sorgic, "Basics of detailed thermal-hydraulic model for thermal design of oil power transformers," *IEEE Trans. Power Del.*, vol. 25, no. 2, pp. 790–802, Apr. 2010.
[7] F. P. Incropera and D. P. DeWitt, *Heat Mass Transfer*, 5th ed. Hoboken, NJ: Wiley, 2002.
[8] I. E. Idelchik, *Handbook of Hydraulic Resistances*. Boca Raton, FL: CRC, 1994.

Marko Sorgic, photograph and biography not available at the time of publication.

Zoran Radakovic, photograph and biography not available at the time of publication.